J. Am. Chem. Soc. 1995, 117, 8745−8756

Structure and Analysis of Helical Tubulate Inclusion Compounds Formed by 2,6-Dimethylbicyclo[3.3.1]nonane-*exo*-2,*exo*-6-diol

Alison T. Ung, Dawit Gizachew, Roger Bishop,* Marcia L. Scudder,* Ian G. Dance, and Donald C. Craig

Contribution from the School of Chemistry, The University of New South Wales, Sydney 2052, Australia

Received February 20, 1995[⊗]

Abstract: The inclusion properties of 2,6-dimethylbicyclo[3.3.1]nonane-*exo*-2,*exo*-6-diol, **1**, the prototype of the helical tubuland family of diol hosts, have been thoroughly investigated. These diols crystallize with a series of spiral hydrogen bonded spines ···OH···OH···OH···OH··· surrounding parallel canals. A total of 40 inclusion compounds of **1** (employing guests containing a wide range of functional group types) have been characterized. These all crystallize in the chiral space group $P3_121$ (or its enantiomorph $P3_221$) with the guests trapped in the canals along *c*. The structures of 12 of these compounds have been determined by X-ray crystallographic methods, showing that the guests exert a strong influence on the detailed structure of the resulting inclusion compound. Increasing guest size can cause a large (4.8%) increase in the unit cell *a* (= *b*) length (canal width) accompanied by a small decrease (0.96%) in *c* direction (canal length). This results in an 8.9% increase in unit cell volume and a dramatic 62% increase in canal cross-sectional area from 15.6 to 25.3 Å^2 across the series of compounds studied. The intermolecular adjustments which permit these changes are examined in detail. Increases in hydrogen bonding distances, or alterations in the molecular bond lengths and angles exhibited by **1**, are insignificant factors. Rather it is the small changes in angles around the hydrogen bonded spines, and the tilt angles of the diols with respect to the canal axis, which are responsible. Considerable variation is observed in the types of interguest arrangement within the canals of the 12 structures. These are explored and rationalized using crystal engineering arguments, but, generally, weak host−guest interactions are the most important intermolecular forces involved within the helical canals. Exceptions to this are observed for guests substituted with halo groups. Samples of guest-free **1** still have the helical tubuland structure unlike some other members of this diol family. Conclusive evidence for the existence of this lattice containing parallel empty canals each with an unobstructed cross-sectional area of about 15.6 Å^2 is presented.

Introduction

The helical tubulands are a group of alicyclic diols (*e.g.* **1**−**3**, Figure 1) which crystallize in the chiral space group $P3_121$ (or its enantiomorph $P3_221$) with a lattice containing parallel helical canals in which guest molecules can be trapped.[1−3] These racemic diols crystallize from solution as conglomerates where each individual crystal is constructed from chirally pure host molecules. This lattice structural type is therefore entirely different from that present in other families of multimolecular or lattice inclusion hosts such as the tetraarylporphyrins,[4] cyclotriveratrylene,[5] tri-*o*-thymotide,[6] or the MacNicol hexahosts.[7] It has superficial parallels with the tubular host lattices present in urea and thiourea inclusion compounds,[8] but the molecular construction of these structures is quite different, and these molecules cannot be developed into a family of hosts.[2]

The structural core of the helical tubuland lattice is a spiral spine of hydroxy hydrogen bonds ···O-H···O-H···O-H···O-H···surrounding a threefold screw axis. This leads, on repetition, to the open three-dimensional hydrogen bonded structures represented in Figure 1. We are interested in the molecular features controlling the formation of these microporous organic lattices, and for some time we have been synthesizing and developing a family of these diol hosts which feature differing canal sizes, shapes, and inclusion properties. The helical tubulands are unique in that the key hydrogen bonded spine motif can be transplanted into new diol molecules thus affording a family of designed compounds[1−3] with canal cross-sectional areas ranging from 0 to 35 Å^2.

The first example of these compounds that we discovered was 2,6-dimethylbicyclo[3.3.1]nonane-*exo*-2,*exo*-6-diol, **1**. This substance contains parallel canals with an unobstructed triangular cross-sectional area of roughly 20 Å^2 and readily forms lattice inclusion compounds (termed helical tubulates). In this

---

* Please address editorial correspondence to: Dr. Roger Bishop, School of Chemistry, The University of New South Wales, Sydney 2052, Australia. FAX 61-2-662-2835 (till Sept 30, 1995); FAX 61-2-385-6141 (after October 1, 1995); Direct TEL61-2-385-4656; E-mail ORGANIC_OFFICE@GMQ. CHEM. UNSW. EDU. AU.

[⊗] Abstract published in *Advance ACS Abstracts*, August 1, 1995.

[1] Bishop, R.; Dance, I. G. *Inclusion Compounds*; Atwood, J. L., Davies, J. E. D., MacNicol, D. D., Eds.; Oxford University Press: Oxford, 1991; Vol. 4, Chapter 1, pp 1−26.

[2] Bishop, R.; Dance, I. G. *Top. Curr. Chem.* **1988**, *149*, 137−188.

[3] Bishop, R.; Craig, D. C.; Dance, I. G.; Scudder, M. L.; Ung, A. T. *Supramol. Chem.* **1993**, *2*, 123−131.

[4] Byrn, M. P.; Curtis, C. J.; Goldberg, I.; Hsiou, Y.; Khan, S. I.; Sawin, P. A.; Tendick, S. K.; Strouse, C. E. *J. Am. Chem. Soc.* **1991**, *113*, 6549−6557.

[5] Collet, A. *Inclusion Compounds*; Atwood, J. L., Davies, J. E. D., MacNicol, D. D., Eds.; Academic Press: London, 1984; Vol. 2, Chapter 4, pp 97−121.

[6] Arad-Yellin, R.; Green, B. S.; Knossow, M.; Tsoucaris, G. *Inclusion Compounds*; Atwood, J. L., Davies, J. E. D., MacNicol, D. D., Eds.; Academic Press: London, 1984; Vol. 3, Chapter 9, see pp 278−284.

[7] MacNicol, D. D. *Inclusion Compounds*; Atwood, J. L., Davies, J. E. D., MacNicol, D. D., Eds.; Academic Press: London, 1984; Vol. 2, Chapter 5, pp 123−168.

[8] Takemoto, K.; Sonoda, N. *Inclusion Compounds*; Atwood, J. L., Davies, J. E. D., MacNicol, D. D., Eds.; Academic Press: London, 1984; Vol. 2, Chapter 2, pp 47−67.

0002-7863/95/1517-8745$09.00/0

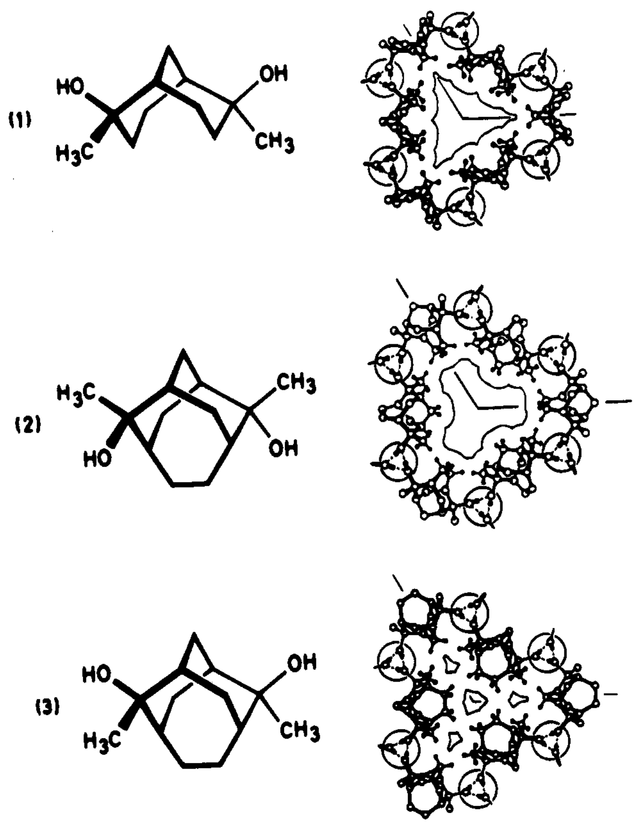

Figure 1. Molecular structures of examples **1**–**3** of the helical tubuland diol family. For each a cross-sectional view in the *ab* plane is shown of one canal only. These projection views are planar representations showing a slice across the helical hydrogen bonded diol arrangement around the canal. Hydrogen bonds are shown as dashed lines and the spines are circled for emphasis. Selected hydrogen atoms are drawn as filled circles to define the van der Waals surface of the canal.

investigation we report the outcome of a detailed screening program conducted with diol **1** and potential guest species. Our aims were to explore the range of guest sizes and functionalities which could be accommodated, the interdependence between host and guest species, and the mechanisms by which the hydrogen-bonded host lattice adapts to guests of different size.

We find that **1** forms inclusion compounds with guests containing a surprisingly diverse range of functionality. Forty inclusion compounds have been prepared and characterized. The structures of 12 of these have been determined by X-ray crystallography and are reported here in full. These guest molecules of differing size and shape can result in significant alteration to the unit cell and canal dimensions but do not cause disruption of the helical tubuland lattice type itself. The crystal structures reveal how this is achieved and also provide significant information about host–guest and guest–guest arrangements within the canals. Evidence is presented demonstrating that the remarkable canal structure of **1** can persist in the guest-free state.

Experimental Section

Synthesis. 2,6-Dimethylbicyclo[3.3.1]nonane-*exo*-2,*exo*-6-diol **1** was prepared as described previously.[9] It was recrystallized twice from acetonitrile or ethyl acetate. The resulting helical tubulate inclusion compound was then sublimed twice under reduced pressure (*ca.* 150 °C/2 mmHg) to yield pure, solvent-free **1**.[10]

Inclusion Compounds. Three preparative procedures were utilized.

Method A. Solvent free **1** (0.05 g, 0.27 mmol) was dissolved with warming in the liquid guest (usually 2–3 mL), and the resulting solution was left to stand at room temperature overnight or with slow evaporation of solvent for a longer period. In a few cases crystals were grown at 0 °C. The needle-like crystals were filtered, allowed to dry in air, and then characterized.

Method B. A limitation of method A is the poor solubility of **1** in certain liquids (notably some hydrocarbons). Method B was as above but using a solution of guest in mesitylene (which is too bulky to be included).

Method C. As for method A, but using a solution of the guest in other solvents. Each sample was checked by IR (mull) and ^1H NMR spectroscopy (Bruker AC300, 300 MHz) in d_6-DMSO solution (where appropriate) to confirm the presence of guest species. An X-ray powder diffraction pattern (XRPD; Siemens D500 instrument; Cu-Kα radiation λ = 1.5418 Å) was then recorded to confirm the presence of the host helical tubuland lattice. Values are quoted here as XRPD 2θ degrees (relative intensity). Single crystal X-ray structures, elemental analysis, and NMR integration values were used (as indicated) to determine the stoichiometry. Solid state ^{13}C MAS and Bloch decay NMR spectra were obtained on a Bruker MSL300 instrument. Determination of the stoichiometry used the integral of peak areas obtained using a 60 s recycle delay time.[11]

Stoichiometry Based on Single Crystal X-ray Results. Method C; $(\mathbf{1})_3$·(acetonitrile): Diol crystallized from a mixture of guest and 1,1,2-trichlorotrifluoroethane; XRPD 8.7 (54), 15.0 (62), 15.3 (77), 19.6 (33), 21.4 (6), 22.8 (22), 26.1 (9), 28.9 (8), 29.5 (5), 30.1 (9), 34.4 (8).

A; $(\mathbf{1})_3$·(1,2-dimethoxyethane)$_{0.75}$: XRPD 8.5 (100), 14.8 (100), 15.2 (47), 15.9 (18), 19.4 (29), 22.5 (65), 25.9 (11), 28.8 (10), 29.7 (42), 30.8 (10), 34.2 (8). Found: C, 70.87, H, 11.15. $(C_{11}H_{20}O_2)_3$·$(C_4H_{10}O_2)_{0.75}$ requires C, 70.75; H, 10.95.

A; $(\mathbf{1})_3$·(1,2-dichloroethane)$_{0.75}$: XRPD 8.25 (98), 14.45 (100), 15.0 (38), 16.7 (13), 19.2 (22), 22.25 (39), 25.70 (12), 28.5 (11), 29.4 (21), 30.6 (9).

A; $(\mathbf{1})_3$·(ethyl acetate): XRPD 8.4 (15), 14.6 (100), 15.2 (34), 16.9 (30), 19.4 (28), 22.4 (74), 25.8 (10), 28.5 (13), 29.4 (27). Found: C, 69.26; H, 10.62. $(C_{11}H_{20}O_3)_3$·$(C_4H_8O_2)$ requires C, 69.34; H, 10.69.

B; $(\mathbf{1})_3$·(chloroacetic acid)$_{1.2}$: XRPD 8.4 (48), 14.6 (69), 15.2 (58), 16.8 (19), 19.4 (39), 21.2 (7), 22.3 (43), 25.8 (11), 28.4 (12), 29.4 (25), 30.6 (6), 34.1 (9), 39.5 (8).

A; $(\mathbf{1})_3$·(propanoic acid)$_{1.2}$: XRPD 8.4 (63), 14.2 (19), 14.6 (100), 15.2 (50), 16.7 (20), 16.8 (20), 19.4 (30), 22.3 (58), 25.7 (14), 28.4 (9), 29.3 (16), 30.5 (10).

A; $(\mathbf{1})_3$·(trichloroethene)$_{0.86}$: XRPD 8.2 (62), 14.35 (100), 14.9 (60), 16.55 (5), 19.2 (29), 20.95 (4), 22.2 (29), 25.5 (11), 28.2 (13), 29.2 (10), 30.15 (7), 33.9 (7).

A; $(\mathbf{1})_3$·(thiophene): XRPD 8.1 (43), 14.2 (100), 15.0 (30), 16.4 (28), 19.0 (15), 21.8 (49), 25.2 (7), 27.8 (7), 28.7 (11), 29.8 (9). Found: C, 68.46; H, 10.37. $(C_{11}H_{20}O_2)_3$·(C_4H_4S) requires C, 68.24; H, 10.59.

A; $(\mathbf{1})_3$·(chlorobenzene): XRPD 8.2 (44), 14.2 (85), 15.2 (51), 16.4 (23), 19.1 (29), 21.8 (37), 25.3 (9), 27.9 (9), 28.7 (12), 29.9 (10), 33.8 (6).

A; $(\mathbf{1})_3$·(toluene)$_{0.86}$: XRPD 8.2 (75), 14.15 (100), 15.05 (69), 16.3 (22), 19.05 (44), 21.7 (44), 25.2 (17), 27.8 (13), 28.55 (17), 29.85 (14).

A; $(\mathbf{1})_3$·(dioxane): XRPD 8.3 (100), 13.6 (12), 14.3 (60), 14.6 (13), 15.0 (41), 16.3 (11), 16.5 (17), 19.1 (47), 22.0 (25), 25.4 (8), 28.1 (6), 28.9 (15), 33.9 (8). Found: C, 68.95; H, 10.80. $(C_{11}H_{20}O_2)_3$·$(C_4H_8O_2)$ requires C, 69.34; H, 10.69.

Stoichiometry Based on Single Crystal X-ray and ^1H NMR Data. C; $(\mathbf{1})_3$·(diiodine)$_{0.5}$·(ethanol)$_{0.5}$: Diol crystallized from a solution of guest in ethanol. XRPD 8.4 (36), 14.5 (51), 15.1 (43), 16.8 (10), 19.3 (27), 21.1 (5), 22.4 (20), 25.4 (5), 25.8 (8), 28.5 (7), 29.5 (11), 34.2 (11).

Analytical and XRPD data for the following 28 inclusion compounds (which were characterized but not studied by single crystal X-ray crystallography) is listed in the supporting information. Here, only the preparative procedure and stoichiometry $(\mathbf{1})_3$·(guest)$_x$ are given.

---

[9] Dance, I. G.; Bishop, R.; Hawkins, S. C.; Lipari, T.; Scudder, M. L.; Craig, D. C. *J. Chem. Soc., Perkin Trans. 2* **1986**, 1299–1307.

[10] Ung, A. T.; Bishop, R.; Craig, D. C.; Dance, I. G.; Scudder, M. L. *J. Chem. Soc., Chem. Commun.* **1991**, 1012–1014.

[11] Gizachew, D. Ph.D. Thesis, UNSW, 1994. Gizachew, D.; Van Gorkom, L. C. M.; Dance, I. G.; Hanna, J. V.; Wilson, M. A. *Solid State Nucl. Mag. Res.* **1994**, *3*, 67–78.

Stoichiometry Based on Elemental Analysis. A, $(\mathbf{1})_3\cdot$(acetic acid)$_{1.0}$; A, (formamide)$_{1.5}$; A, (*N*-methylformamide)$_{1.5}$; A, (ethylbenzene)$_{0.6}$; A, (*p*-xylene)$_{0.5}$; A, (*m*-xylene)$_{0.6}$; A, (cyclohexene)$_{0.5}$; A, (diethylamine)$_{0.5}$; A, (mesityl oxide)$_{0.5}$; A, (acetone)$_{1.5}\cdot$(water)$_{1.5}$; A, (dimethyl sulfoxide)$_{1.71}$; A, (bromobenzene)$_{0.5}$; A, (*m*-dichlorobenzene)$_{0.65}$; C, (1,3-dibromopropane)$_{0.43}$; A, (chloroform)$_{0.86}$; B, (ethyl 2-bromopropanoate)$_{0.5}$; A, (2,5-dibromothiophene)$_{0.42}$.

Stoichiometry Based on ^{1}H NMR Spectroscopy. C, (1,2-dicyanoethane)$_{0.75}$; A, (tetrahydrofuran)$_{0.86}$; A, (ethanol)$_{1.12}$; A, (1-butanol)$_{0.6}$; A, (benzene)$_{0.75}$; B, (3-bromopropanoic acid)$_{0.6}$.

Stoichiometry Based on ^{13}C NMR Spectroscopy. A, (tetrachloroethylene)$_{0.72}$; A, (bromotrichloromethane)$_{0.88}$; A, (3,4-dichloro-1,2,5-thiadiazole)$_{0.88}$; A, (1,4-dichlorobutane)$_{0.60}$; A, (2,5-dichlorothiophene)$_{0.60}$.

Guest molecules apparently are not included by **1**: *o*-dichlorobenzene, cyclohexanone, *o*-xylene, and *trans*-1,2-dibromocyclohexane.

Solution and Refinement of the X-ray Structures. For each of the 12 structures, data were recorded using an Enraf Nonius CAD4 X-ray diffractometer. Numerical details pertaining to the collection of data, data processing, and refinement of the structures are given in Table 1. Procedures adopted for data collection and processing have been described.[12] An alternative absorption correction procedure[13] was used for the 1,2-dichloroethane and chlorobenzene inclusion compounds.

The first of these structures to be examined was the ethyl acetate inclusion compound. The solution of this structure has been described and coordinates published.[9] The diol molecule has C_2 symmetry and is positioned on a twofold axis in space group $P3_121$. At the time, it was not possible to locate the individual atoms of the guest molecule. The positional parameters for the diol molecule determined from this structure analysis were used as input for the initial Fourier calculations for each compound described here.

The space group symmetry which creates the fascinating helical tubuland host lattice makes location of the guest molecule difficult. The guest molecule is situated along and near the *z* axis. This coincides with the threefold screw axis, and there are twofold axes separated by *c*/6 (*ca.* 1.17 Å) perpendicular to it. Guest molecules do not conform to these symmetry requirements and are necessarily disordered. Difference Fourier maps are therefore difficult to interpret as they contain a superposition of six symmetry related guest molecules. It should also be noted that, unlike host–guest compounds involving coordination or filled cages, there may be no strict requirement for either stoichiometric or commensurate host–guest behavior in these helical tubulate compounds.

Modeling of the guest started with the assignment of the largest peak in the difference map as one atom. The model was then slowly built up by including other peaks (or their symmetry related equivalents) which gave geometry appropriate for the guest. For some guests, *e.g.*, chlorobenzene or trichloroethylene, the geometry is fixed, and the whole guest molecule can be defined once part of it has been assigned. For other guest molecules, *e.g.*, ethyl acetate or 1,2-dimethoxyethane (monoglyme), there are torsion angles to be taken into account. In these cases, computer modeling of the guest gave ranges of possible interatomic distances. When sufficient atom positions had been assigned to fix all or part of the guest molecule, a rigid group was incorporated for that part of the molecule. When the entire guest molecule had been included, refinement of its position and orientation were carried out. In some cases individual atom positions were refined, but they were slack constrained to maintain reasonable geometry.

The occupancy of the guest was allowed to vary. For $P3_121$ (or $P3_221$) there are six equivalent positions in the unit cell, so an occupancy of 0.1667 (1/6) for the guest leads to a stoichiometry of $(\mathbf{1})_3\cdot(\text{guest})_1$ for the inclusion compound and one guest molecule per unit cell. Other values of the occupancy which could be represented as $1/n$ (for n near to 6) lead to packing of the guests within the canal which can be described with a finite repeat unit. For example, for $n = 7$, there is 6/7 of a guest molecule per unit cell, and so there are six guest molecules along seven unit cell lengths. For convenience of describing these systems, the occupancies of the guest molecules were set to the nearest value of $1/n$. This gave a stoichiometry of $(\mathbf{1})_3\cdot(\text{guest})_{6/n}$ for the inclusion compound. When $n = 6$ adjacent guest molecules are related by a unit cell translation in the *z* direction. When $n \neq 6$, adjacent guest molecules are related by other symmetry elements. For each structure it was necessary to ensure that the arrangement of adjacent guest molecules did not lead to unreasonably short guest–guest contacts.

Before inclusion of the guest molecule in the refinement, the *R* factor for data with $\sin \theta/\lambda < 0.1$ was invariably high. These data are particularly sensitive to omitted electron density and are a valuable measure of the progress of the refinement. We have used R_{low} to represent *R* for these very low angle data. When the guest molecule was included in the refinement, R_{low} dropped markedly.

For all structures, the refinement of the atoms of the host diol molecule was carried out anisotropically. The position of the hydroxy hydrogen atom was determined from a difference map, and its position was refined. All other H atoms were included in calculated positions and were not refined. These were assigned isotropic temperature factors equivalent to those of the atoms to which they were bound. Refinement was carried out using program RAELS[14] which has rigid group refinement capabilities, the ability to apply slack constraints to a model, and also allows for the refinement of twinned specimens. The occupancy of the guest was initially allowed to vary for each structure. For the final stages of refinement, the occupancy was set to a value (of $1/n$) which was near the refined value and which gave interguest contacts which were reasonable and was not refined.

Full details of the processes of location and refinement of the guest molecule for each structure are given in the supporting information. A brief summary is given below, with four residuals quoted being *R* and R_{low} for the final structure and *R* and R_{low} for the structure after omission of the guest.

Acetonitrile Compound. A difference Fourier map calculated from the published positional parameters[9] for the diol showed a series of peaks along the *z* direction, the distance between them being appropriate for an acetonitrile molecule. The molecule was therefore included in the structure as a rigid group. The occupancy was 0.1667 (1/6). Refinement converged with $R = 0.031$ (0.050; 0.053, 0.16).

1,2-Dimethoxyethane (Monoglyme) Compound.[15] The host structure was refined anisotropically to give $R = 0.079$. A difference map computed at this stage contained three peaks in the region where the guest was expected to be. A geometry calculation including all symmetry for these three peaks showed that it was possible to construct a chain of six atoms which were approximately the correct distance apart and at approximately the correct angular relationships to represent a monoglyme molecule. These six atoms were introduced into the refinement with the C–O distances slack constrained to 1.43 Å and the C–C distance to 1.54 Å. All the angles in the guest molecule were lightly constrained to 109.5°. The occupancy of the monoglyme molecule was 0.125 (1/8), resulting in three monoglyme molecules for every four unit cells of the host. Refinement converged with $R = 0.032$ (0.058; 0.071, 0.30).

Diiodine Compound.[15] The positional parameters from $\mathbf{1}^9$ were used as input for the initial Fourier calculations in space group $P3_121$. This gave $R = 0.303$. Introduction of two I atoms at the positions of the largest peaks on the difference map dropped *R* only to 0.284. Preliminary refinement gave $R = 0.207$, but the temperature factors of the host atoms were not realistic. Comparative refinement showed that the incorrect enantiomer had been selected. When the coordinates of the atoms were transformed to $-x, -y, -z$ and the space group was changed to $P3_221$, refinement proceeded normally and converged with $R = 0.035$ (0.055; 0.212, 0.46). The occupancy of the I_2 molecule was 0.0833 (1/12), so there was one complete I_2 molecule for two unit cells of the host.

1,2-Dichloroethane Compound. A difference Fourier calculated from the published positional parameters[9] for the diol showed one dominant residual peak positioned along the *z* axis. Molecular modeling was used to determine the range of Cl···Cl distances in 1,2-

---

(12) Herath Banda, R. M.; Dance, I. G.; Bailey, T. D.; Craig, D. C.; Scudder, M. L. *Inorg. Chem.* **1989**, *28*, 1862–1871.

(13) De Meulenaer, J.; Tompa, H. *Acta Crystallogr.* **1965**, *19*, 1014–1018.

(14) Rae, A. D. *RAELS, A Comprehensive Constrained Least-Squares Refinement Program*; University of New South Wales, 1989.

(15) A preliminary description of this compound has appeared: Ung, A. T.; Bishop, R.; Craig, D. C.; Dance, I. G.; Scudder, M. L. *J. Chem. Soc., Perkin Trans. 2* **1992**, 861–862.

Table 1. Numerical Details of the Solution and Refinement of Structure for Helical Tubulate Compounds of **1**

formula, formula mass	$(C_{11}H_{20}O_2)_3\cdot(CH_3CN)$	$(C_{11}H_{20}O_2)_3\cdot(C_4H_{10}O_2)_{0.75}$	$(C_{11}H_{20}O_2)_3\cdot(I_2)_{0.5}$	$(C_{11}H_{20}O_2)_3\cdot(C_2H_4Cl_2)_{0.75}$	$(C_{11}H_{20}O_2)_3\cdot(C_4H_8O_2)$	$(C_{11}H_{20}O_2)_3\cdot(ClC_2H_3O_2)_{1.2}$	$(C_{11}H_{20}O_2)_3\cdot(C_3H_6O_2)_{1.2}$	$(C_{11}H_{20}O_2)_3$-$(C_2HCl_3)_{0.86}$	$(C_{11}H_{20}O_2)_3\cdot(C_4H_4S)$	$(C_{11}H_{20}O_2)_3\cdot(C_6H_5Cl)$	$(C_{11}H_{20}O_2)_3\cdot(C_7H_8)_{0.86}$	$(C_{11}H_{20}O_2)_3\cdot(C_4H_8O_2)$
molecular weight	593.89	620.43	679.75	627.06	640.95	666.24	641.73	665.28	636.98	665.40	631.82	640.95
crystal description	(0−10)(110) (−20−3)(1−11) (011)(−101) (1−20)(−210) (100)(−100) (1−10)(−110)	{100}(00−1) (−101) (1−11)(011)	{100}{101}	{100}(00−1) (101)(1−11) (0−11)(−101) (−111)(011)		{100}{001}	{100}{001}	{001}{100}	{100}{001}	{001}{100}	{001}(1−10) (−210) (−100)(100) (010)(0−10)	{100}{001}
space group	$P3_121$	$P3_121$	$P3_221$	$P3_121$	$P3_121$	$P3_121$	$P3_121$	$P3_121$	$P3_121$	$P3_121$	$P3_121$	$P3_121$
a, b/Å	11.8990(7)	12.0416(3)	12.068(2)	12.0745(5)	12.165(1)	12.180(1)	12.1832(5)	12.284(2)	12.4083(5)	12.455(1)	12.469(2)	12.4699(5)
c/Å	7.0274(4)	7.0110(2)	6.984(3)	6.9868(5)	7.001(1)	6.9725(8)	6.9746(2)	6.980(1)	6.9702(4)	6.960(1)	6.961(1)	6.9687(4)
V/Å^3	861.67(7)	880.39(4)	880.8(4)	882.15(7)	897.3(2)	895.8(1)	896.54(5)	912.2(2)	929.39(6)	935.0(2)	937.3(2)	938.43(6)
temp/°C	21(1)	21(1)	21(1)	21(1)	21(1)	21(1)	21(1)	21(1)	21(1)	21(1)	21(1)	21(1)
Z	1	1	1	1	1	1	1	1	1	1	1	1
D_{calc}/g cm^{-3}	1.14	1.17	1.28	1.18	1.19	1.23	1.19	1.21	1.14	1.18	1.12	1.13
radiation, λ/Å	CuKα, 1.5418	CuKα, 1.5418	MoKα, 0.7107	CuKα, 1.5418	CuKα, 1.5418	CuKα, 1.5418	CuKα, 1.5418	CuKα, 1.5418	CuKα, 1.5418	CuKα, 1.5418	CuKα, 1.5418	CuKα, 1.5418
μ/cm^{-1}	5.70	5.99	9.34	16.26		14.73	6.23	23.3	10.58	12.31	5.42	5.86
crystal dimensions/mm	~0.15 × 0.10 × 0.35	0.27 × 0.21 × 0.30	0.07 × 0.12 × 0.20	~0.11 × 0.12 × 0.40		0.07 × 0.07 × 0.47	0.08 × 0.09 × 0.30	~0.10 × 0.08 × 0.27	0.22 × 0.21 × 0.46	0.08 × 0.08 × 0.48	~0.09 × 0.09 × 0.54	0.21 × 0.13 × 0.53
scan mode	$\theta/2\theta$	$\theta/2\theta$	$\theta/2\theta$	$\theta/2\theta$	$\theta/2\theta$	$\theta/2\theta$	$\theta/2\theta$	$\theta/2\theta$	$\theta/2\theta$	$\theta/2\theta$	$\theta/2\theta$	$\theta/2\theta$
$2\theta_{max}$, deg	140	140	50	140		140	140	120	140	140	120	140
ω scan angle	0.60 + 0.15tan θ	0.60 + 0.15tan θ	0.50 + 0.35tan θ	0.60 + 0.15tan θ		0.60 + 0.15tan θ	0.60 + 0.15tan θ	0.60 + 0.15tan θ	0.60 + 0.15tan θ	0.60 + 0.15tan θ	0.60 + 0.15tan θ	(0.60 + 0.15tan θ)
no. of intensity measurements	3280	3347	3110	3346		3359	3368	2627	3544	3585	2743	3590
criterion for obs reflcn	$I/\sigma(I) > 3$	$I/\sigma(I) > 3$	$I/\sigma(I) > 3$	$I/\sigma(I) > 3$	$I/\sigma(I) > 3$	$I/\sigma(I) > 3$	$I/\sigma(I) > 3$	$I/\sigma(I) > 3$	$I/\sigma(I) > 3$	$I/\sigma(I) > 3$	$I/\sigma(I) > 3$	$I/\sigma(I) > 3$
no. of independent obsd reflcns	1028	1083	709	1029	605	923	975	774	1029	1002	854	1123
no. of refl (m) and variables (n) in final refinement	1028, 77	1083, 96	709, 81	1029, 81	605, 87	923, 84	975, 84	774, 82	1029, 80	1002, 75	854, 79	1123, 81
$R = \sum^m\lvert\Delta F\rvert/\sum^m\lvert F_o\rvert$	0.031	0.032	0.035	0.038	0.041	0.041	0.033	0.041	0.026	0.051	0.028	0.036
$R_w = [\sum^m w\lvert\Delta F\rvert^2/\sum^m w\lvert F_o\rvert^2]^{1/2}$	0.040	0.042	0.041	0.050	0.047	0.048	0.039	0.045	0.031	0.068	0.033	0.048
$s = [\sum^m w\lvert\Delta F\rvert^2/(m-n)]^{1/2}$	2.40	2.89	1.60	2.90	4.18	2.29	1.97	2.08	2.01	3.40	1.79	2.97
crystal decay	none	none	1 to 0.74	1 to 0.75		1 to 0.87	none	1 to 0.75	none	1 to 0.90	none	1 to 0.97
max, min transmission coeff	0.94, 0.84	0.90, 0.85	0.93, 0.80	0.86, 0.67		0.91, 0.71	0.96, 0.89	0.84, 0.76	0.82, 0.63	0.92, 0.71	0.97, 0.92	0.93, 0.83
R for multiple measurements	0.013	0.011	0.031	0.013		0.017	0.017	0.021	0.014	0.016	0.017	0.014
largest peak in final diff map/e Å^{-3}	0.14	0.12	0.28	0.27	0.40	0.26	0.13	0.35	0.17	0.23	0.15	0.25

dichloroethane as the Cl−C−C−Cl dihedral angle was varied. The large peak and a twofold related equivalent of it were the appropriate distance apart to be the two chlorine atoms of the guest when in the staggered conformation. This peak was included in the refinement along with a carbon atom, which, with its twofold related counterpart, would complete the guest molecule. The asymmetric unit of the guest molecule was therefore only half of the molecule with a twofold axis relating its two halves. Slack constraints were implemented to maintain reasonable geometry for the guest molecule. The occupancy of the guest molecule was 0.125 (1/8). Refinement converged with $R = 0.038$ (0.078; 0.077, 0.30).

Ethyl Acetate Compound. After the previously published refinement,[9] there was one large residual peak in the difference Fourier map. A carbon atom was introduced into the model at this position. Careful inspection of the resulting difference map, along with consideration of all possible symmetry related peaks, gave some indication of positions for the atoms of the planar acetate group. This part of the guest molecule was introduced into the refinement as planar and rigid. This led to further improvement in R and in particular in R_{low}. The residual peaks in the next difference map which were close to the proposed O atoms of the model were then considered individually; calculations eliminated some possibilities when the peak positions were too close to the walls of the host lattice. Eventually, it was possible to propose a model which fitted within the canal and was geometrically reasonable. Slack constraints were imposed to retain sensible geometry for the ethyl group and to ensure that it did not refine to a position which was too close to the canal walls. The occupancy of the guest molecule was 0.1667 (1/6). Refinement converged with $R = 0.041$ (0.163; 0.065, 0.58). This compares with the previously published refinement for which $R = 0.049$ using limited data with $\sin\theta/\lambda > 0.3$.

Chloroacetic Acid Compound. After preliminary refinement of the host structure, $R = 0.099$. A difference map at this stage showed one dominant peak, so this peak was included in the refinement as a chlorine atom. It seemed likely that pairs of chloroacetic acid molecules would be hydrogen bonded together along the inclusion canal, in the manner frequently observed for carboxylic acids. Computer modeling was used to determine the range of intermolecular Cl$\cdots$Cl distances for which guest molecules would adopt this hydrogen bonding pattern. It was found that an appropriate distance would exist if pairs of guest molecules were related by one of the twofold axes penetrating the canal. The remainder of the guest molecule was modeled as four coplanar atoms with appropriate bond distances and angles. The C−Cl distance was slack constrained to be 1.70 Å, and the O$\cdots$O hydrogen bonding distances were slack constrained to be 3.0 Å. The two carboxyl groups hydrogen bonded together were slack constrained to be coplanar. There were two possible arrangements for the carboxyl groups with respect to the twofold axis relating them; the twofold axis could be either in the plane of the carboxyl groups or perpendicular to it. Both possibilities were tested, and the model with the twofold axis perpendicular to the plane of the carboxyl groups refined to 0.041 compared with 0.048 for the alternate model. The occupancy of the chloroacetic acid molecule was 0.2 (1/5), representing six molecules per five unit cell lengths of canal. Refinement converged to give $R =$ 0.041 (0.053; 0.093, 0.41). The R factor for the other enantiomer was 0.042.

Propanoic Acid Compound. After the successful refinement of the chloroacetic acid inclusion compound it was considered likely that propanoic acid would occupy the canal in the host lattice in a very similar way. The model for the chloroacetic acid guest refinement was incorporated into the refinement of this structure (with the chlorine atom being replaced by CH_3-). The resulting refinement was good, with the residual dropping to 0.036. The CH_3-CH_2 distance was slack constrained to be 1.54 Å, and the O$\cdots$O hydrogen bonding distances were slack constrained to be 3.0 Å. The two carboxyl groups hydrogen bonded together were slack constrained to be coplanar. The occupancy of the propanoic acid molecule was 0.2 (1/5), as for the chloroacetic acid host−guest system. Refinement converged to give $R = 0.033$ (0.074; 0.055, 0.31).

Trichloroethene Compound. Structure factors calculated using the published positional parameters for the diol[9] gave $R = 0.28$. It was not until a twinned model (incorporating h,k,l and $-h-k,k,l$) was adopted that a satisfactory R factor was obtained for the host structure alone (reducing R to 0.094). At this stage a difference Fourier map was computed. It was possible to find symmetry related copies of the three largest peaks in the difference map which were at approximately the correct distances and orientation to be the three chlorine atoms of the guest. The complete guest molecule was then overlaid over these peaks and included in the model as a rigid group. The occupancy of the guest molecule was 0.1429 (1/7). Refinement converged with R = 0.041 (0.080; 0.082, 0.38). The twin components, whose sum was maintained at 1.0, refined to 0.569(3) and 0.431.

Thiophene Compound.[15] Preliminary refinement of the host gave $R = 0.244$. Inspection of the data indicated that the crystal was probably twinned; with equivalent data h,k,l and $-h-k,k,l$. When a 50−50 twin was introduced, R immediately fell to 0.055. A difference map at this stage did not show one dominant peak, so the thiophene was included as a freely disordered plate with bond lengths of 1.54 Å (the weighted mean of S−C and C−C). The occupancy of the guest was 0.1667 (1/6). Refinement converged to give $R = 0.026$ (0.087; 0.039, 0.34).

Chlorobenzene Compound. The largest peak in a difference Fourier calculated from the published positional parameters for the diol[9] was positioned along the z axis. This was included as a chlorine atom. It was then possible to find in a subsequent difference Fourier, peaks which began to define the position and orientation of the benzene ring. The guest was introduced as a rigid group, overlaid on those peaks. The occupancy of the guest molecule was 0.1667 (1/6) so that there was one guest molecule per unit cell. Refinement converged with R = 0.051 (0.067; 0.066, 0.37).

Toluene Compound. It was necessary to invoke a twinned model (incorporating h,k,l and $-h-k,k,l$) in order to obtain a satisfactory R factor for the host structure alone. At this stage a Fourier map revealed parts of the toluene guest. These atoms were included in the refinement, and eventually it was possible to overlay a complete toluene molecule against peaks in the Fourier map. The guest was then included in the structure as a rigid group. Occupancy of the toluene was 0.1429 (1/7). Refinement converged with $R = 0.028$ (0.082; 0.041, 0.29). The two twin components were constrained to have a sum of 1 and refined to 0.649(2) and 0.351.

Dioxane Compound. The positional parameters from **1**[9] were used as input for the initial Fourier calculations. A difference map at this stage showed several small residual peaks which could be linked together to form part of a six-membered ring. Computer modeling was used to generate orthogonal coordinates for a typical dioxane molecule in the chair conformation. These coordinates were overlaid on the difference map peaks to generate a dioxane molecule as a rigid group; the assignment of the two oxygen atoms being arbitrary. After some refinement it was found that one of the atoms which had been assigned as carbon was only about 3.2 Å from the wall of the canal. The carbon/oxygen assignment of the atoms of the ring was therefore changed so that this atom was oxygen (and therefore capable of closer contact to the wall of the canal). However, the assignment of carbon and oxygen atoms in the dioxane rings is by no means unequivocal and is probably of no consequence as far as the refinement of the structure is concerned. The occupancy of the dioxane molecule was 0.1667. Refinement converged to give $R = 0.037$ (0.127; 0.049, 0.38).

Guest-Free Diol 1. Method A. The helical tubulate inclusion compound of **1** with acetonitrile or ethyl acetate was sublimed twice under reduced pressure (*ca.* 150 °C/2 mmHg) to yield pure, solvent-free **1**[10] (Found: C, 72.03; H, 11.18. $C_{11}H_{20}O_2$ requires C, 71.70, H, 10.90).

Method B. The helical tubulate was heated (*ca.* 100 °C) under reduced pressure (2 mmHg) (Found: C, 71.64; H, 11.02. $C_{11}H_{20}O_2$ requires C, 71.70, H, 10.90).

Method C. The helical tubulate or guest-free diol was recrystallized from mesitylene (Found: C, 72.00; H, 11.07. $C_{11}H_{20}O_2$ requires C, 71.70, H, 10.90).

Samples prepared by all three methods were identical by elemental analysis, IR (mull) spectroscopy, and X-ray powder diffraction pattern.

Vapor Absorption by Diol 1. Samples of powdered guest-free **1** were left exposed to vapor of acetone, chloroform, or ethyl acetate in a sealed container at room temperature until saturation was achieved. IR (mull) spectra were recorded to monitor the extent of absorption.

Table 2. Crystallographic Dimensions of Helical Tubulate Inclusion Compounds of Diol **1** Determined from Single Crystal X-ray Structural Determination[a]

compound	$a = b$ (Å)	c (Å)	V (Å^3)	UCA (Å^2)	O···O (Å)	*C*−*O*H···*O* (deg) (donor)	*C*−*O*···H*O* (deg) (acceptor)	*O*H···*O*H···*O*H (deg)	tilt angle (deg)
(**1**)$_3$·(acetonitrile)	11.8990(7)	7.0274(4)	861.67(7)	15.6	2.812	107.8	129.3	122.7	65.6
(**1**)$_3$·(1,2-dimethoxyethane)$_{0.75}$	12.0416(3)	7.0110(2)	880.39(4)	17.7	2.808	107.9	128.9	122.6	66.8
(**1**)$_3$·(diiodine)$_{0.5}$·(ethanol)$_{0.5}$	12.068(2)	6.984(3)	880.8(4)	18.1	2.804	108.4	128.6	122.3	66.7
(**1**)$_3$·(1,2-dichloroethane)$_{0.75}$	12.0745(5)	6.9868(5)	882.15(7)	18.1	2.804	108.2	128.7	122.4	66.7
(**1**)$_3$·(ethyl acetate)	12.165(1)	7.001(1)	897.3(2)	19.8	2.808	108.5	128.0	122.4	67.3
(**1**)$_3$·(chloroacetic acid)$_{1.2}$	12.180(1)	6.9725(8)	895.8(1)	19.8	2.805	108.6	128.3	122.0	67.3
(**1**)$_3$·(propanoic acid)$_{1.2}$	12.1832(5)	6.9746(2)	896.54(5)	19.9	2.805	108.6	128.1	122.0	67.4
(**1**)$_3$·(trichloroethylene)$_{0.86}$	12.284(2)	6.980(1)	912.2(2)	21.9	2.809	109.2	127.2	122.0	67.9
(**1**)$_3$·(thiophene)	12.4083(5)	6.9702(4)	929.39(6)	24.3	2.814	109.2	126.9	121.5	68.4
(**1**)$_3$·(chlorobenzene)	12.455(1)	6.960(1)	935.0(2)	24.9	2.816	109.5	126.3	121.2	68.5
(**1**)$_3$·(toluene)$_{0.86}$	12.469(2)	6.961(1)	937.3(2)	25.1	2.813	109.3	126.4	121.4	68.4
(**1**)$_3$·(dioxane)	12.4699(5)	6.9687(4)	938.43(6)	25.3	2.817	109.4	126.2	121.3	68.5

[a] UCA is the unobstructed cross-sectional area of the host canal when drawn as a projection in the *ab* plane. O···O is the interoxygen separation in the hydrogen bonded spine of the diol host lattice. The next three columns describe intermolecular angles present in the hydrogen bonded spine of the host lattice. Tilt angle is the angle C2···C6···z axis, where C2 and C6 are the carbons bearing the hydroxy groups and z is the canal direction.

The materials produced were found to be identical to the helical tubulates obtained by crystallization.

Results and Discussion

Scope of Helical Tubulate Formation. All 40 inclusion compounds investigated are believed to have the helical tubuland structure on the basis of their similar X-ray powder diffraction patterns. The guests studied encompass a very wide range of organic functionality, but this has no effect on the efficacy of the formation of the host lattice. Acids, bases, nonpolar, polar, and protic compounds are all equally accommodated, and guests capable of hydrogen bonding do not interfere with the host hydrogen bonding network. The potent inclusion capabilities of diol **1** therefore do not depend on interactions with specific types of guest structures. Rather it will act as a host for most organic guests with the appropriate size and shape for entrapment within its canals.

The only guest structural type found to be an exception is the phenol functionality which can give rise to an alternative cocrystalline lattice type. In crystallization experiments with phenols helical tubuland diols are either recovered in pure condition, or, in some cases, a stoichiometric intimately hydrogen bonded lattice structure is obtained.[16,17] A full account of 16 such compounds (including seven single crystal X-ray structures) has been published recently.[18] Diol **1** forms compounds of this type with phenol, *o*-, *m*-, and *p*-chlorophenol, and with hydroquinone.

Some helical tubuland diols (*e.g.*, **2**)[19] can yield hydrate structures in which the water and diol molecules are intimately hydrogen bonded together. Careful study of **1** revealed no such tendency.

As noted in the Experimental Section a variety of methods was used to assign the host−guest stoichiometry for the various compounds. While these techniques were in rough agreement with each other, they did not agree exactly. Single crystal X-ray determinations sometimes indicated a slightly higher guest content than the bulk sample methods used. Although the use of ^{13}C MAS−NMR peak integrals can be uncertain because of the long relaxation times of carbon in the solid state, the host−guest ratios obtained with 60 s recycle delay time accorded well with those found from X-ray crystallography,[11] for example, for the 1,2-dichloroethane compound 3:0.75 (X-ray) and 3:0.71 (MAS−NMR); trichloroethylene compound 3:0.86 in both cases; and the toluene compound 3:0.86 (X-ray) and 3:0.77 (MAS−NMR). Elemental analysis tended to indicate slightly different amounts of guest than the other methods. These slight disparities are a common problem in the characterisation of inclusion compounds where the two components are associated only by van der Waals forces and have incongruent symmetry which may result in non-stoichiometric ratios.

Dimensional Variation within the Helical Tubuland Host Lattice Structure. The crystallographic determinations reveal that the helical tubuland lattice of diol **1** has more flexibility to accommodate particular guests than might have been anticipated. Table 2 lists the 12 structures in order of their increasing $a = b$ values. These dimensions, which control the canal cross-sectional area, range from 11.8990(7) Å for the acetonitrile compound to 12.4699(5) Å for the dioxane compound. Thus an increase of 0.571 Å or 4.8% is observed across the range of compounds studied. The change is accompanied by a general (but not exact) trend to a decreasing value for c (*i.e.*, along the canal axis) from 7.0274(4) Å to 6.960(1) Å. This represents a decrease of 0.067 Å or 0.96% across the series of compounds examined.

Thus the canals exhibit significant elasticity by increasing their cross-section; but there is only a small concomitant decrease in their length. The net effect on the unit cell volume (V) is an almost perfect correlation with increasing values from 861.67(7) Å^3 for the acetonitrile compound to 938.43(6) Å^3 for the dioxane case. This represents an increase of 76.76 Å^3 or 8.9% across the series.

However, because of the significant changes in the values of a ($= b$), the most dramatic alteration is the canal unobstructed cross-sectional area (UCA). This changes from 15.6 (for acetonitrile guest) to 25.3 Å^2 (for dioxane guest) across the series of compounds, a remarkable increase of 9.7 Å^2 or 62%.

The UCA is analogous to the view seen looking along an indented pipe. It is a good, but not perfect, measure of the true cross-section at any particular position since it is the result of a flat projection of a three-dimensional helical array. Since the internal surfaces of the canals are not smooth, the individual UCA values represent the minimum cross-sectional canal area which is available for guest occupation in each compound.

Factors Controlling the Canal Dimensional Changes. The obvious question arising from the previous section is just how are these observed structural changes achieved? One possibility

---

[16] Ung, A. T.; Bishop, R.; Craig, D. C.; Dance, I. G.; Scudder, M. L. *J. Chem. Soc., Chem. Commun.* **1993**, 322−323.

[17] Bishop, R.; Craig, D. C.; Dance, I. G.; Scudder, M. L.; Ung, A. T. *Mol. Cryst. Liq. Cryst.* **1994**, *240*, 113−119.

[18] Ung, A. T.; Bishop, R.; Craig, D. C.; Dance, I. G.; Scudder, M. L. *Chem. Materials* **1994**, *6*, 1269−1281.

[19] Hawkins, S. C.; Bishop, R.; Dance, I. G.; Lipari, T.; Craig, D. C.; Scudder, M. L. *J. Chem. Soc., Perkin Trans. 2* **1993**, 1729−1735.

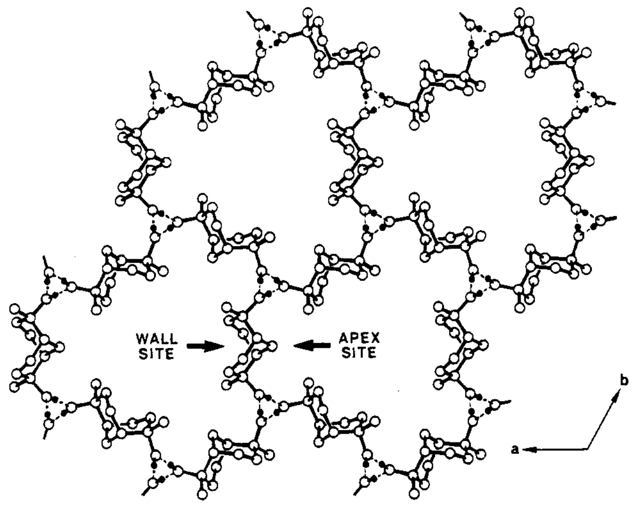

Figure 2. The structural relationship between the apex and wall sites occupied by diol **1** in adjacent canals. Apex and wall diols in any one canal play the opposite role in the adjacent canals. Hydrocarbon hydrogens are omitted for clarity. The hydroxy hydrogens are shown as filled circles and hydrogen bonds as dashed lines.

would be that the hydrogen bonds of the spines simply stretch to accommodate increasing sizes of guest as observed, for example, in cage clathrates of 4-*p*-hydroxyphenyl-2,2,4-trimethylthiachroman.[20] However, this idea is not supported by the values of O···O obtained from the crystal structures. Values cover the small range 2.804–2.817 Å, without any obvious trend being apparent (Table 2). This observation suggests that this hydrogen bonding distance is important for producing the energy minimum and that little distortion is tolerated in the various structures. Similarly, although molecules of **1** have some potential conformational flexibility, there are no significant variations in the interatomic distances, bond angles, or torsion angles observed from the crystallographic data (see supporting information).

On the other hand, several trends are apparent in the *angles* associated with the spine hydrogen bonding. For example, the values for *C*–*O*H···*O* show a trend to increase (107.8–109.5°) with increasing values of *a*. In contrast the values of *C*–*O*···H*O* (129.3–126.2°) and O···O···O (122.7–121.2°) show a trend to decrease as *a* increases (Table 2).

Molecules of **1** surrounding any canal have two distinct different orientations (Figure 2). Either the C9 methylene bridge (the apex site) or the *endo*-surface (the wall site) of the diol faces inwards. These sites are reversed in the adjacent canal: *i.e.*, the apex site of one canal is the wall site of the next and *vice versa*. A superimposed projection view of the smallest (acetonitrile guest) and largest (dioxane guest) canals is shown in Figure 3. The consequent surprising observation is that for any one canal the apex sites remain almost unchanged in position, while the large increase in canal size results from the wall sites being displaced outwards. Since these roles are reversed in neighboring canals the net effect is lattice expansion in the *ab* plane.

As shown in Figure 4, the effect is for the two spines subtended from any one diol molecule to swing outwards away from the C9 methylene bridge with a concomitant tightening of the spine angles. Thus, the three diol apex sites in any one canal only change position slightly, while the three diol wall sites move outwards significantly. Because of the crystal symmetry the net increased separation between an apex and a wall site is the increase in *a* (and *b*) length.

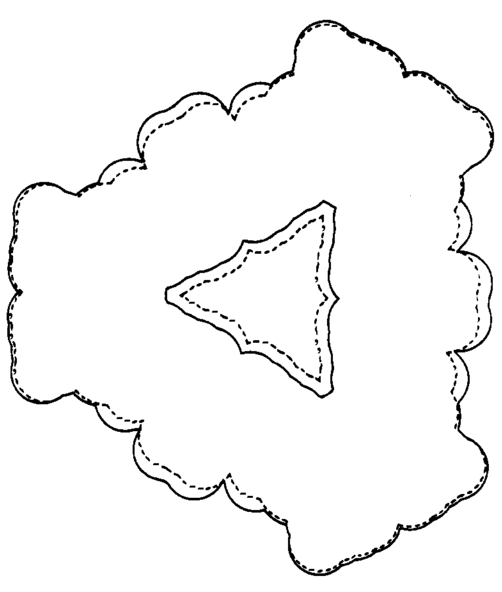

Figure 3. Projections in the *ab* plane of the inner and outer surfaces of one canal each of $(\mathbf{1})_3$·(acetonitrile) (drawn as dashed lines) and $(\mathbf{1})_3$·(dioxane) (drawn as solid lines) to the same scale and superimposed. These represent the smallest (15.6 Å^2) and largest (25.3 Å^2) unobstructed canal cross-sections obtained from X-ray crystallographic data. Comparison with Figure 2 shows that the canal apex sites occupy essentially the same positions in each case but that the wall sites move outwards in the larger case.

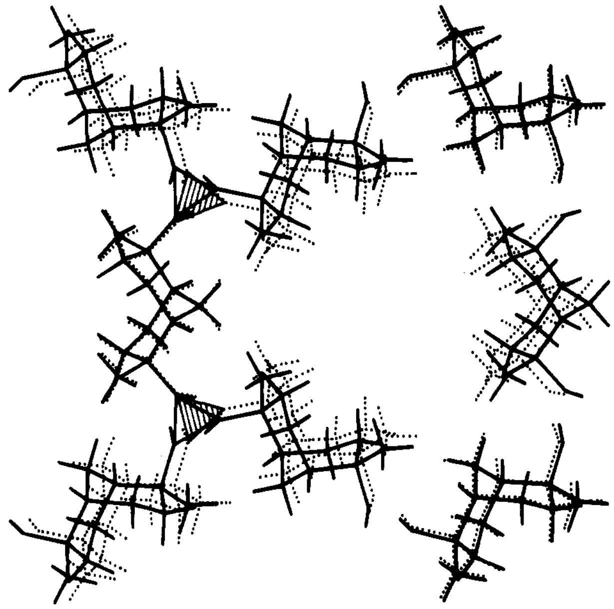

Figure 4. An alternative representation of the superimposed canals of the $(\mathbf{1})_3$·(acetonitrile) and $(\mathbf{1})_3$·(dioxane) inclusion compounds shown in Figure 3 but showing the positional change of the helical spines (hatched to open triangles) as the guest size increases. In any one canal the diol apex sites occupy essentially the same locations, but the wall sites are displaced outwards.

A further trend observed is for the diol molecules to alter their orientation (tilt angle) with respect to the *z* axis. As *a* increases, the angle which C2···C6 (the carbons bearing the hydroxy groups) makes with the *z* axis increases from 65.6° for the acetonitrile compound to 68.5° for the dioxane case (see Table 2). In other words the molecule is able to become less tilted as *a* increases. This accounts for the small but systematic decrease in *c* as *a* increases.

While these individual trends are small, in concert they are sufficient to bring about the large observed dimensional changes. Hence minor angular changes in the hydrogen bonding spines,

---

[20] Hardy, A. D. U.; McKendrick, J. J.; MacNicol, D. D.; Wilson, D. R. *J. Chem. Soc., Perkin Trans. 2* **1979**, 729–734.

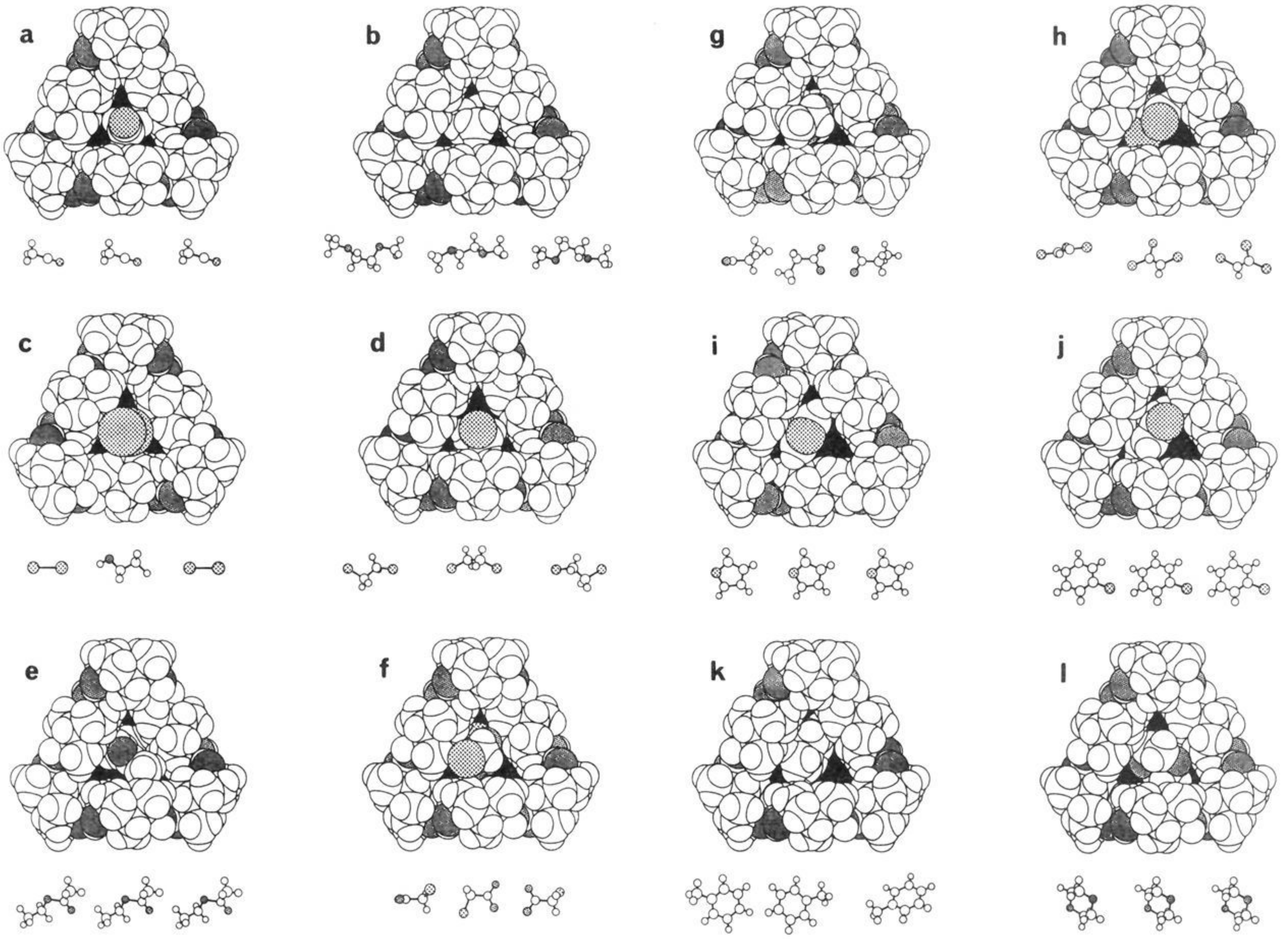

Figure 5. Projection views along *c* for one canal only of each of the 12 inclusion compounds examined by single crystal X-ray crystallography. Each is drawn to the same scale showing one molecule of guest in a typical orientation: (a) acetonitrile, (b) 1,2-dimethoxyethane, (c) iodine/ethanol, (d) 1,2-dichloroethane, (e) ethyl acetate, (f) chloroacetic acid, (g) propanoic acid, (h) trichloroethene, (i) thiophene, (j) chlorobenzene, (k) toluene, and (l) dioxane. The unoccupied space in each canal has been filled to emphasize the guest. Under each canal projection view typical orientations of the guest molecules along the canal are also shown. These guests are drawn to the same scale as each other and are represented here with the *c* axis horizontal.

together with a change in the tilt of the molecules, provide a surprisingly efficient method for the apparently inflexible network of diol molecules to expand in the *ab* plane without significant change to the hydrogen bond length.

Host–Guest and Guest–Guest Packing Arrangements. It was pointed out previously that the guest molecules in all the inclusion compounds are disordered, and hence their positions and orientations are known with relatively low precision. The separation of adjacent guest molecules within the canal was determined from the crystallographic occupancy of the guest. Once again there is uncertainty in this figure although all values used gave good *R* factors and relatively good R_{low} values. In addition, they did not result in unreasonably short guest–guest contacts. In the following discussion we try to interpret our results in terms of the arrangement of guest molecules, their interaction with each other, and with the canal. The low precision for the guest positions should be borne in mind.

Figure 5 shows a section through one canal only for each of the 12 inclusion compounds studied by single crystal X-ray methods. These projection views in the *ab* plane (drawn to the same scale) show the various guest molecules located in the canals. The arrangement of the guest molecules along the canal is shown in each case below the projection. Here the canal axis *z* is horizontal.

Each compound is now discussed individually. Comparisons are drawn here with previously reported structures and crystal engineering[21] features of significance.

Acetonitrile Compound (Figure 5a). The guest molecules are aligned at a slight angle to the *z* axis. Since the occupancy of the guest is 1/6, the stoichiometry is $(\mathbf{1})_3$·(acetonitrile), and there is one acetonitrile molecule per unit cell length. Adjacent molecules are related by one cell translation. In this case there are no significant host–guest or guest–guest interactions. The guest molecules are presumably prevented from moving within the canal by weak C–H···H host–guest attractive forces. It is noteworthy that the –CN stretching vibration expected around 2300 cm^{-1} is not observed in the IR (mull) spectrum of this compound, perhaps reflecting the lack of polarizability in this environment.

Acetonitrile is included by many other host molecules, for example, as a clathrate within the hydroquinone structure.[22] In a number of cases these host–guest combinations were stabilized by significant intermolecular interactions.[23]

1,2-Dimethoxyethane (Monoglyme) Compound (Figure 5b). The occupancy of 1/8 leads to a stoichiometry of $(\mathbf{1})_3$·(monoglyme)$_{0.75}$ and three guest molecules occupying four unit cell lengths within the canal. Adjacent guest molecules are related by crystallographic symmetry other than pure translation. It is possible to propose two different arrangements of guest molecules, both of which are consistent with stoichiometry and

---

(21) Desiraju, G. R. *Crystal Engineering: The Design of Organic Solids*; Elsevier: Amsterdam, 1989.

(22) Chan, T.-L.; Mak, T. C. W. *J. Chem. Soc., Perkin Trans. 2* **1983**, 777–781.

(23) For example: Vögtle, F.; Berscheid, R.; Schnick, W. *J. Chem. Soc., Chem. Commun.* **1991**, 414–416. de Boer; J. A. A.; Reinhoudt, D. N.; Harkema, S.; van Hummel, G. J.; de Jong, F. *J. Am. Chem. Soc.* **1982**, *104*, 4073–4076. Gilmore, C. J.; MacNicol, D. D.; Murphy, A.; Russell, M. A. *Tetrahedron Lett.* **1983**, *24*, 3269–3272.

neither of which leads to guest−guest contacts which are too short. One arrangement is shown in Figure 5b which represents four unit cell lengths. The shortest intermolecular C···C distances are both 4.0 Å. In the other arrangement, the repeat unit is eight unit cells containing six guest molecules. The two different intermolecular distances are 3.7 and 4.4 Å. It is not known if one arrangement is preferred to the other or if they both occur (in different canals). Projected in the *ab* plane, the monoglyme guest is situated compactly in the center of the canal with several CH groups near to the canal wall. Monoglyme is accommodated in the canal by twisting to fit snugly around the bumps in the wall.

Diiodine Compound (Figure 5c). Since the occupancy is 1/12 there is one iodine per two unit cells of the host. This results in an I···I separation of 11.4 Å, whereas the sum of the van der Waals radii is only 4.3 Å. The implication was that some other species was also present in the canal, and solution ^{1}H NMR spectra in d_6-acetone and d_6-DMSO confirmed the presence of ethanol solvent (quartet *ca.* 3.5 δ). Integration indicated an overall stoichiometry of $(\mathbf{1})_3\cdot(\text{diiodine})_{0.5}\cdot(\text{ethanol})_{0.5}$. The coguest was not revealed by the X-ray structure determination, but the structure contains sufficient space to accommodate ethanol. A modeled arrangement of the guest ethanol is presented in the figure.

Relatively few crystal structures of inclusion compounds containing diiodine (as opposed to polyiodide species) have been reported. α-Cyclodextrin·I_2·$4H_2O$ has the element present within cages where it is stabilized by O···I−I···O interactions[24] and the hexakis(2,6-di-*O*-methyl)-α-cyclodextrin·I_2 inclusion compound has a rather similar arrangement.[25] Our material appears to be the first report of discrete I_2 units being included in a tubular host structure. Only poor CH···I_2 interactions are possible between host and guest, and this is presumably the driving force for coinclusion of ethanol solvent. Coordination between oxygen and iodine yielding a series of 1:1 coguest units along the canals provides the necessary energetic stabilization for the compound.

1,2-Dichloroethane Compound (Figure 5d). As for the monoglyme compound, the occupancy of 1/8 leads to a stoichiometry of $(\mathbf{1})_3\cdot(\text{1,2-dichloroethane})_{0.75}$. Guest molecules align themselves along the *z* axis. The shortest host−guest C···C interaction is 3.9 and 4.1 Å for Cl···C. The shortest distance between Cl atoms of adjacent guest molecules is 5.3 Å suggesting that in this instance Cl···Cl interactions[26] are not significant in stabilizing the interguest arrangement within the canal. The asymmetric unit of the guest comprises half the molecule. The refined value of the Cl−C−C−Cl dihedral angle was 127°. This value is presumably preferred over the classical 180° staggered conformation, because it fits better within contours of the canal.

Ethyl Acetate Compound (Figure 5e). The occupancy of 1/6 corresponds to a stoichiometry of $(\mathbf{1})_3\cdot(\text{ethyl acetate})$ and adjacent guest molecules being related by simple unit cell translation. The shortest guest−guest C···C distance is 4.1 Å. Ethyl acetate fits within a relatively small canal (a = 12.165 Å), being able to follow the contours of the wall by suitable modification of the C−C−O−CO and C−O−CO−C torsion angles.

Chloroacetic Acid Compound (Figure 5f). The occupancy of 0.2 corresponds to a stoichiometry of $(\mathbf{1})_3\cdot(\text{chloroacetic acid})_{1.2}$. Chloroacetic acid molecules are present in the canal as hydrogen bonded dimers with a twofold axis perpendicular to the plane containing the carboxyl groups. Hence both chlorine atoms are oriented toward one wall of the host canal, whereas the four oxygen atoms of the dimer lie in a plane roughly parallel to one of the canal walls. There is a Cl···Cl contact of 3.86 Å between chlorines of neighboring dimers, thus indicating weak guest−guest interaction.[26]

Pure chloroacetic acid has been reported to exist in three crystalline arrangements,[27] of which the crystal structures of two have been determined. The stable α-form is a cyclic hydrogen bonded tetramer,[28] the metastable β-form is the cyclic centrosymmetric dimer,[29] and the polymeric catemer is believed to be disfavored because of a short C−Cl···O contact in such a potential structure. It is obvious that the tetramer could not be accommodated within the helical tubulate canals of **1** hence the observation of a dimer, albeit not the one normally encountered. This example is a good reminder that the constraints imposed by host lattices may well result in different guest arrangements to those normally considered in the free state.

Propanoic Acid Compound (Figure 5g). The occupancy of 0.2 indicates six guest molecules per five unit cells or a stoichiometry of $(\mathbf{1})_3\cdot(\text{propanoic acid})_{1.2}$. As for the chloroacetic acid compound, the carboxylic acid molecules are present in the canal as hydrogen bonded dimers with a twofold axis perpendicular to the plane containing the carboxyl groups. A hydrogen bonded dimer is produced which fits along one edge of the host canal with both methyl groups oriented toward this wall.

Propanoic acid has been enclathrated by the scissor-shaped 1,1′-binaphthyl-2,2′-dicarboxylic acid host[30] where it was present as the centrosymmetric dimer which is frequently the stable form of carboxylic acids.[31] However, in other cases it has been found to coordinate with polar host groups as a complex.[32]

Trichloroethene Compound (Figure 5h). The occupancy of 1/7 gives a stoichiometry of $(\mathbf{1})_3\cdot(\text{trichloroethene})_{0.86}$ with six guest molecules occupying seven unit cell lenths of canal. Alternate guest molecules have the opposite orientation. The shortest host−guest distances are Cl···C of 3.6 Å, while between guests the shortest Cl···Cl distances[26] are 3.8 and 4.5 Å. Hence, both host−guest and guest−guest interactions play a part in stabilizing this compound.

Thiophene Compound (Figure 5i). The occupancy of 1/6 leads to a stoichiometry of $(\mathbf{1})_3\cdot(\text{thiophene})$ and adjacent guest molecules being related by unit cell translation. The thiophene guest molecule is positioned along one edge of the host canal, presumably because this is the region where there is most space. It was not possible to distinguish between sulfur and carbon atoms in the crystallographic study so the sulfur position is random over the five possibilities. The shortest interguest C/S···C/S distance is 4.5 Å.

Although thiophene is a less commonly used guest it is known to be included in thiourea channels.[33] It also has been reported to form 1:1 inclusion compounds with triphenylmethane[34] and

---

[24] James, W. J.; French, D.; Rundle, R. E. *Acta Crystallogr.* **1959**, *12*, 385−389. McMullan, R. K.; Saenger, W.; Fayos, J.; Mootz, D. *Carbohydrate Res.* **1973**, *31*, 211−227.

[25] Harata, K. *Chem. Lett.* **1986**, 2057−2060.

[26] Sarma, J. A. R. P.; Desiraju, G. R. *Acc. Chem. Res.* **1986**, *19*, 222−228.

[27] Aumeras, M.; Minangoy, R. *Bull. Soc. Chim. Fr.* **1948**, *15*, 1100−1107.

[28] Kanters, J. A.; Roelofsen, G. *Acta Crystallogr., Sect. B* **1976**, *32*, 3328−3331. Kanters, J. A.; Roelofsen, G.; Feenstra, T. *Acta Cryst., Sect. B* **1976**, *32*, 3331−3333.

[29] Sinha, D.; Katon, J. E.; Jakobsen, R. J. *J. Mol. Str.* **1975**, *24*, 279−291.

[30] Csöregh, I.; Czugler, M.; Weber, E.; Ahrendt, J. *J. Inclus. Phenom.* **1990**, *8*, 309−322.

[31] Leiserowitz, L. *Acta Cryst., Sect. B* **1976**, *32*, 775−802.

[32] Csöregh, I.; Finge, S.; Weber, E. *Bull. Chem. Soc. Jpn.* **1991**, *64*, 1971−1975. Toda, F.; Kai, A.; Tagami, Y.; Mak, T. C. W. *Chem. Lett.* **1987**, 1393−1396.

other hosts where intermolecular heteroatom interactions are effective.[35]

Chlorobenzene Compound (Figure 5j). The occupancy of 1/6 leads to a stoichiometry of $(\mathbf{1})_3$·(chlorobenzene) and adjacent guest molecules being related by unit cell translation. It might have been expected that Cl··Cl interactions[26] would result in chlorobenzene molecules associating in a head to head fashion but this was not the case. Instead, the guest molecules lie along the *z* axis with the C−Cl bond tilted towards one side of the canal. There is a short guest−guest contact of 3.2 Å for C··Cl (and 2.4 Å for C−H··Cl). The shortest host−guest C··C interactions are 3.9 and 4.1 Å for Cl··C. It has been reported previously that C−H··Cl hydrogen bonds are an alternative favorable attraction for chloro compounds[36] and that these are preferred for aromatic (rather than aliphatic) hydrogen atoms.[37]

Toluene Compound (Figure 5k). There are six molecules occupying seven unit cell lengths of canal since the guest occupancy is 1/7. The stoichiometry is $(\mathbf{1})_3$·(toluene)$_{0.86}$. Unlike the chlorobenzene guest, adjacent toluene molecules alternate in orientation. This means that methyl groups point toward each other, with the C··C distance being 5.2 Å. The shortest aryl−aryl C··C distance is 3.6 Å, and the shortest host−guest distances are 3.6 Å. Since the volumes[38] of chloro (*ca.* 19.9 Å^3) and methyl (*ca.* 23.5 Å^3) groups are comparable, it would be surprising that the chlorobenzene and toluene cases differ in guest orientation were it not for the C−H··Cl attractions described above.

Dioxane Compound (Figure 5l). The occupancy of 1/6 leads to a stoichiometry of $(\mathbf{1})_3$·(dioxane) and adjacent guest molecules being related by unit cell translation. The dioxane molecules have been modeled as adopting the normal chair conformation. The shortest guest−guest C··C or O··O are 5.3 Å.

Dioxane is a particularly efficacious molecule for producing inclusion compounds because of its ability to participate in both conventional −O-H··O hydrogen bonding[39] and the weaker −C-H··O host−guest hydrogen bonding.[40,41] In all the cases reported dioxane exists in the expected chair conformation.

In summary, for most of the 12 inclusion compounds investigated, there is little evidence of significant guest−guest interactions which might result in major stabilization of these compounds. The exceptions are those with halo-substituted guests. Of the four inclusion compounds containing chlorine there is a relatively short Cl··Cl distance of 3.8 Å in the trichloroethylene compound and 3.9 Å in the case of chloroacetic acid. Furthermore, chlorobenzene exhibits a short Cl··C distance of 3.2 Å, and diiodine as guest is stabilized by coinclusion of ethanol. It seems that the other helical tubulate compounds are stabilized primarily by weak C−H··H host−guest contacts and that guest−guest interactions are generally a secondary consideration.

Guest-Free Diol 1. The structures of microporous solids such as **1**−**3** beg the question as to the potential stability of the host lattice in the absence of guest molecules. When known host compounds are prepared free of guests, the normal situation is for a nonporous phase to result. This is particularly true if the building blocks are small organic molecules associated only through weak forces. For example, while urea and thiourea form many inclusion compounds of the tubuland type, the pure hosts have entirely different crystal packing arrangements without void spaces.[8] The alternative situation where empty cavities or canals are retained is rare. However, Dianin's compound which has a cage structure is reported to retain this arrangement in unsolvated form,[42] and it is widely appreciated that more robust microporous solids such as zeolites can retain their structural integrity on guest removal.[43] Recently, the organic host gossypol has also been reported as crystallizing with large open canals.[44]

For **3** the free spaces in the canals are too small for inclusion and therefore there is little question that these are genuinely empty voids within the solid structure.[9] Guest-free samples of **2** exhibit a quite different XRPD pattern to the inclusion compounds. This indication of a different lattice type has been confirmed by single crystal X-ray work which showed that a new layer structure without voids was produced.[10] What of the canals formed by diol **1**?

Guest-free samples of **1** were produced by sublimation under reduced pressure, by heating the helical tubulate inclusion compounds under reduced pressure, and by crystallization from mesitylene (see Experimental Section). The composition and structure of the resulting material was examined by IR (mull) spectroscopy and elemental analysis. All three preparative procedures gave identical material with microanalyses compatible with the value calculated for pure $C_{11}H_{20}O_2$. The IR spectra of guest-free **1** and helical tubulates of **1** were virtually identical apart from the guest peaks (Figure 6). Notably there were no significant changes in the O−H stretching region which might have implied a different hydrogen bonding arrangement.

^{13}C cross-polarization and magic angle spinning solid state NMR studies[11] showed that the carbon resonances observed for the guest-free diol were almost the same as for the helical tubulate compounds, except for slight changes in δ up to 1 ppm. This also indicates that the lattice structure of the host is largely unchanged in the two cases.

Microcrystalline solvent-free **1** grown from mesitylene solution was found by flotation to have a density of 0.99 g cm^{-3}, since at 20 °C the material sank slowly when suspended in *N*-methylaniline (d = 0.985 g cm^{-3}) but rose very slowly when suspended in water (d = 0.998 g cm^{-3}). This result should be compared to the value (1.02 g cm^{-3}) calculated for the empty helical tubuland lattice and the range of values (1.12−1.28 g cm^{-3}) calculated for the 12 X-ray structures listed in Table 1.

Exposure of guest free **1** to vapor led to absorption with formation of the helical tubulate materials (see Experimental Section). Spontaneous formation of inclusion compounds from exposure of pure host to guest vapor is well-established in certain cases, for example, in the canal-containing cyclophos-

---

[33] Brown, J. F. Jr.; White, D. M. *J. Am. Chem. Soc.* **1960**, *82*, 5671−5678.

[34] Hartley, H.; Thomas, N. G. *J. Chem. Soc.* **1906**, 1013−1033.

[35] MacNicol, D. D.; Swanson, S. *Tetrahedron Lett.* **1977**, 2969−2972. Cobb, R. L. *U. S. Pat.* 3,998,853, Dec. 21, 1976 & 4,039,541, Aug. 2, 1977 (Phillips Petroleum Co.); (*Chem. Abstr.* **1977**, *86*, 139824r & **1977**, *87*, 152046d).

[36] Taylor, R.; Kennard, O. *J. Am. Chem. Soc.* **1982**, *104*, 5063−5070.

[37] Perutz, M. F.; Fermi, G.; Abraham, D. J.; Poyart, C.; Bursaux, E. *J. Am. Chem. Soc.* **1986**, *108*, 1064−1078; see especially p 1076.

[38] Kitaigorodsky, A. I. *Molecular Crystals and Molecules*; Academic Press: New York, 1973.

[39] MacNicol, D. D.; Mallinson, P. R. *J. Inclus. Phenom.* **1983**, *1*, 169−174. Csöregh, I.; Weber, E.; Nassimbeni, L. R.; Gallardo, O.; Dörpinghaus, N.; Ertan, A.; Bourne, S. A. *J. Chem. Soc., Perkin Trans. 2* **1993**, 1775−1782.

[40] Desiraju, G. R. *Acc. Chem. Res.* **1991**, *24*, 290−296.

[41] Pich, K. C.; Bishop, R.; Craig, D. C.; Scudder, M. L. *J. Inclus. Phenom.* **1994**, *18*, 149−160.

[42] MacNicol, D. D. *Inclusion Compounds*; Atwood, J. L., Davies, J. E. D., MacNicol, D. D., Eds.; Academic Press: London, 1984; Vol. 2, Chapter 1, pp 1−45.

[43] Barrer, R. M. *Inclusion Compounds*; Atwood, J. L., Davies, J. E. D., MacNicol, D. D., Eds.; Academic Press: London, 1984; Vol. 1, Chapter 6, pp 191−248.

[44] Ibragimov, B. T.; Talipov, S. A.; Aripov, T. F. *J. Inclus. Phenom.* **1994**, *17*, 317−324.

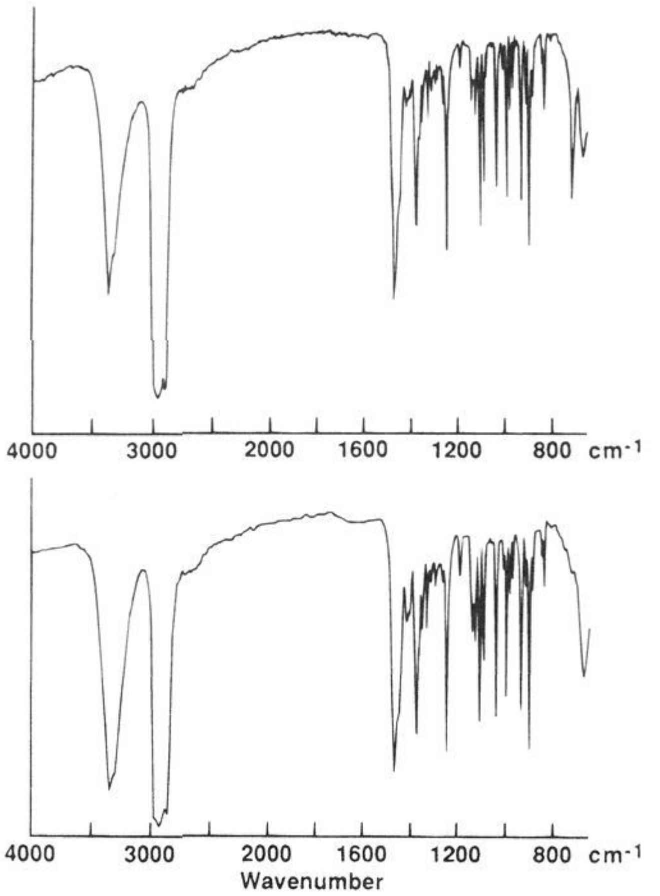

Figure 6. Comparison of the paraffin mull infrared spectra of (top) the helical tubulate inclusion compound $(\mathbf{1})_3$•(thiophene), and (bottom) solvent-free diol **1**.

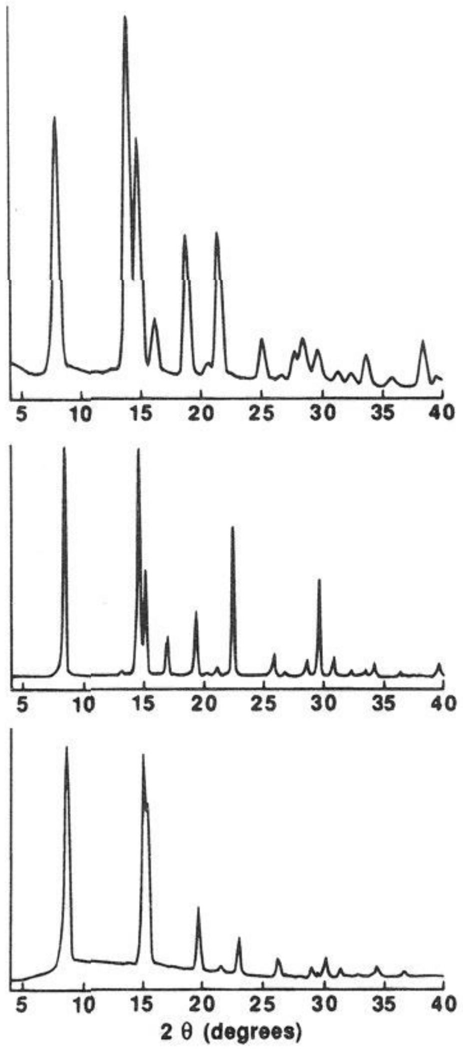

Figure 7. Comparison of the X-ray powder diffraction patterns (from top to bottom) of the two helical tubulate inclusion compounds $(\mathbf{1})_3$•(toluene)$_{0.86}$ and $(\mathbf{1})_3$•(1,2-dimethoxyethane)$_{0.75}$, plus the solvent-free diol **1**. These illustrate examples of large, small, and the smallest possible, canal cross-sectional areas.

phazene series,[45] the Werner hosts,[46] and recently for cholic acid and methyl cholate.[47]

Unfortunately the quality of crystalline **1** produced by the methods described above has been inadequate to permit definitive study by single crystal X-ray techniques, but XRPD analysis confirms that guest-free diol **1** retains its porous canal structure.

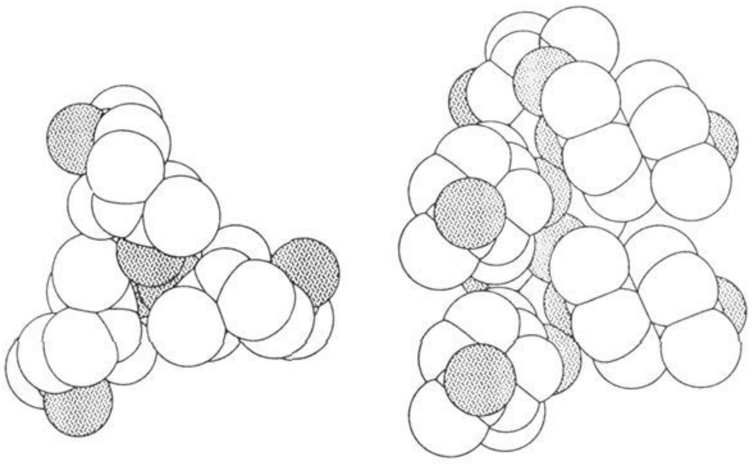

Figure 8. Part of the helical hydrogen bonded spine structure of diol **1** molecules, shown in space-filling representation, which comprises the structural core of the helical tubuland lattice. Left: projection close to the *ab* plane showing the trigonal arrangement with eclipsed columns of diol molecules. Right: the same substructure with the *c* axis vertical. Hydrogen atoms are omitted for clarity. Oxygen atoms are stippled.

Powder Diffraction Information. Diol **2** forms either ellipsoidal clathrate or helical tubulate compounds depending on the size and shape of the guest used.[3] When the guest is too large for either lattice type, guest free **2** is obtained.[10] Each of these three crystal forms has a distinctive powder pattern, so for diol **2**, powder diffraction (XRPD) proves to be an invaluable tool in determining the nature of the inclusion compounds produced.

For diol **1**, however, with the exception of certain small phenols as guests,[17] only powder patterns typical of helical tubulate compounds are observed. The question as to whether an inclusion compound has been formed or not with a particular guest can be determined by careful interpretation of the XRPD data. Typical XRPD patterns are shown in Figure 7. Predominant peaks are at approximately 8.3, 14.5, 15.2, 16.5, 19.2, and 22.4° in 2θ. The peaks at 8.3 and 16.5° are the *100* and *200* reflections. As the guest size increases, these reflections move to lower 2θ values consistent with an increase in a (and b). However, eventually a limit in guest size is reached above which the lattice can no longer accommodate the potential guest. The helical tubuland lattice is retained but is empty with a (and b) smaller, and the *100* and *200* reflections in the XRPD reflect this change. The *100* reflection moves to 8.6°, and the *200* reflection becomes very weak (as can be calculated from any of the single crystal analyses if the guest is omitted). Typical values are as follows:

guest	*100* reflection	*200* reflection
acetonitrile	8.6	–
monoglyme	8.5	17.0
ethyl acetate	8.4	16.9
p-xylene	8.3	16.5
thiophene	8.1	16.4
o-dichlorobenzene	8.6	–(not included)
o-xylene	8.6	–(not included)

The XRPD of guest-free diol **1** obtained by sublimation has *100* at 8.6 and *200* is not observed (Figure 7). So the only limitation in the use of XRPD as a probe for determining the existence or otherwise of diol **1** inclusion compounds occurs for very small guests, where the pattern is the same as that for guest-free diol **1**. Other physical techniques (such as IR and

---

[45] Allcock, H. R. *Inclusion Compounds*; Atwood, J. L., Davies, J. E. D., MacNicol, D. D., Eds.; Academic Press: London, 1984; Vol. 1, Chapter 8, pp 351–374.

[46] Lipkowski, J. *Inclusion Compounds*; Atwood, J. L., Davies, J. E. D., MacNicol, D. D., Eds.; Academic Press: London, 1984; Vol. 1, Chapter 3, pp 59–103.

[47] Scott, J. L. *J. Chem. Soc., Perkin Trans. 2* **1995**, 495–502.

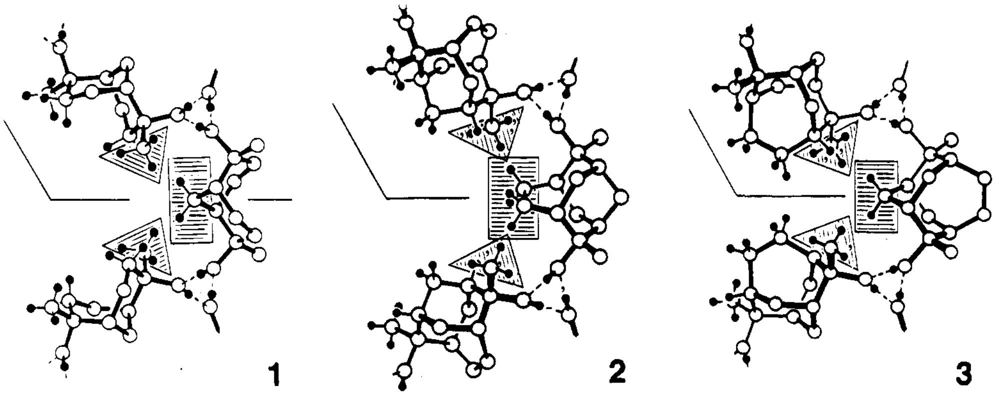

Figure 9. A section of the canal wall of diols **1**−**3** showing adjacent apex bridge and methyl groups highlighted by hatching. It is believed that for diols **1** and **3** these substructures act as molecular keystones which protect the structure against collapse of the canal in the absence of solvent.

NMR) must be used to confirm the existence of inclusion compounds in these cases.

In another experiment, the inclusion compound of cyclohexene with diol **1** gave the typical powder pattern with *100* and *200* at 8.2 and 16.3, respectively. However, when the sample was ground up and the pattern remeasured, the *100* reflection had shifted to 8.6, and *200* had disappeared, indicating that the guest had escaped and the lattice had now adopted the guest-free dimensions. (We have previously observed similar guest loss when samples for IR spectroscopic study were prepared as KBr discs. Consequently we avoid this procedure when investigating inclusion compounds.)

As noted earlier, the a (= b) cell dimension can vary considerably depending on the guest size. From the single crystal diffraction studies reported here, a ranges from 11.899 (for acetonitrile guest) to 12.470 Å (for dioxane). From the positions of the *h00* reflections on the powder patterns of other diol **1**−guest combinations, it is possible to calculate a. The smallest calculated value of a (11.8 Å) corresponds to the sublimed guest free lattice and is very similar to those observed for the inclusion compounds with the smallest guests such as acetonitrile and ethanol. The largest value calculated (12.6 Å) is obtained for the *m*-dichlorobenzene inclusion compound.

In contrast, the c dimension is almost invariate, ranging from 6.96 to 7.03 Å for the single crystal studies performed. In the powder patterns, only the *003* reflection is observed (*001* and *002* being systematically absent) over the 2θ range measured. This reflection is consistently observed at $2\theta = 38.4°$.

Empty Canals in Diol 1. All the above evidence points to the surprising conclusion that diol **1** can exist with empty lattice canals roughly comparable in size to those in the acetonitrile inclusion compound. As discussed earlier, diol **1** has no tendency to form a hydrate structure unlike some other helical tubuland diols (e.g., **2**). Similarly, diols with larger canals (e.g., **2**) are known *not* to retain the helical tubuland structure when guest free.[10] The sum of all this evidence indicates that guest free diol **1** has an especially energetically favorable helical tubuland lattice and is capable of maintaining it without the support of guest molecules or water. Its behavior may be compared to zeolite lattices such as zeolite L and laumontite which have canals along only one axis of the crystal structure.[43]

By its very nature, explanation of such a phenomenon clearly must be largely speculative. The structural core of the host lattice is the helical hydrogen bonded spine, shown in space filling representation in Figure 8. This hydrogen bonding motif is only one of several that we have observed in structures of alicyclic diols. We have already speculated that formation of these various hydrogen bonding types, including the spines, is closely connected with steric factors.[48] Figure 9 shows a section of canal wall for each of the helical tubuland diols **1**−**3**. The volumes of space associated with the methyl groups and the molecular bridge are highlighted. We speculate that as the helical structure develops these groups approach each other. In the case of **3** the canal volume is so small that there is no possibility of its collapse. However, in the absence of guests, diol **2** does indeed adopt an alternative structure. Without stabilization of the large canal volume by solvent molecules the host structure is mechanically unstable. We propose that for the intermediate canal size of diol **1** that interactions between the methyl and bridge volumes lock the canal wall into a stable structure and rule out its collapse. The comparison with construction of an arched bridge assembled from stone blocks springs to mind. Potential instability in such a structure is avoided by locking the arch using a keystone. For diol **1** the methyl groups and bridges act as molecular keystones.

Clearly, in solution, solvation factors will influence the formation of the diol lattice. However, the sublimation result shows that this structure is capable of self-assembly without the involvement of solvents. This is different from the assembly of zeolite lattices where water molecules and aqueous ions are normally required as templates during initial assembly of the host lattice. Thus the molecule **1** is self-programmed to give the microporous structure without the need for intervention by other chemical species. This is a remarkable illustration of the influences that crystal engineering factors[21] can exert in molecular assembly involving small and apparently simple molecules.

Acknowledgment. Financial support is gratefully acknowledged from the Australian Research Council and the Australian International Development Assistance Bureau (scholarship to D.G.).

Supporting Information Available: Elemental analyses and XRPD data for the 28 inclusion compounds not studied by single crystal X-ray crystallography. Further details of refinement and guest location; tables listing positional coordinates, thermal parameters, interatomic distances and angles; and a comparison of diol **1** bond lengths and angles for the 12 crystal structures (39 pages). This material is contained in many libraries on microfiche, immediately follows this article in the microfilm version of the journal, can be ordered from the ACS, and can be downloaded from the Internet; see any current masthead page for ordering information and Internet access instructions.

JA950578M

---

(48) Bishop, R.; Craig, D. C.; Dance, I. G.; Kim, S.; Mallick, M. A. I.; Pich, K. C.; Scudder, M. L. *Supramol. Chem.* **1993**, *1*, 171−178.